7-1-2022

# Guest-Mediated Self-Assembly of Deprotonated 2-Bromoresorcinarenes

Kwaku Twum
*Department of Chemistry, Oakland University, 146 Library Drive, Rochester, Michigan*

Khai-Nghi Truong
*Department of Chemistry, University of Jyvaskyla, Survontie 9 B, Jyväskylä*

Frank Boateng Osei
*Department of Chemistry, Oakland University, 146 Library Drive, Rochester, Michigan*

Carolina von Essen
*Department of Chemistry, University of Jyvaskyla, Survontie 9 B, Jyväskylä*

Sanaz Nadimi
*Department of Chemistry and Biochemistry, University of Windsor, 401 Sunset Avenue, Windsor, Ontario*

*See next page for additional authors*

# Guest-mediated self-assembly of deprotonated 2-bromoresorcinarenes

Kwaku Twum,[a] Khai-Nghi Truong,[b] Frank Boateng Osei,[a] Carolina von Essen,[b] Sanaz Nadimi,[c] John F. Trant,[c] Kari Rissanen[b*] and Ngong Kodiah Beyeh[a*]

[a] *Oakland University, Department of Chemistry, 146 Library Drive, Rochester, Michigan, 48309-4479, USA*

[b] *University of Jyvaskyla, Department of Chemistry, Survontie 9 B, FI-40014 Jyväskylä, Finland*

[c] *University of Windsor, Department of Chemistry and Biochemistry, 401 Sunset Avenue, Windsor, ON, N9B 3P4 Canada*

**ABSTRACT**

Doubly and triply deprotonated 2-bromo-C-alkylresorcinarene anions form host-guest complexes with both tetramethyl ammonium cations and bis-protonated dimethylpiperazine cations. The tri-anion forms a fully closed dimeric capsule with one *endo*- and two *exo*-cavity bis-protonated dimethylpiperazine cations. Interestingly, the di-anion crystallized from a mixture of the 2-bromo-C-methylresorcinarene, dimethylethylenediamine and tetramethylammonium chloride, forms a nanotube consisting of only the 2-bromo-C-methylresorcinarene anion and the tetramethylammonioum cation. The nanotube has an *exo*-functionalized anionic hydrophilic outer

surface that interacts with cationic guests and a hydrophobic interior channel. Solution studies support the deprotonation and the formation of these host-guest complexes. Quantification of binding in chloroform shows a very strong binding constant between the 2-bromo-C-pentylresorcinarene and tetramethylammonioum chloride ($K_1$=3.63×10$^5$ M$^{-1}$, $K_2$=2.32×10$^4$ M$^{-1}$), far higher than observed for the unfunctionalized C-pentylresorcinarene ($K_1$=5.10×10$^4$ M$^{-1}$, $K_2$=1.30×10$^3$ M$^{-1}$). We attribute this to the stronger ion-pair in the former as the halogen increases the acidity of the phenolic hydroxyl groups.

## INTRODUCTION

Resorcinarenes are bowl-shaped cavity-containing calixarene macrocycles (when in the $C_{4v}$ conformation).[1–8] Their modular structure makes them good candidates for functionalization, and consequently useful synthons for constructing complex supramolecular architectures.[6,9–14] Their shallow hydrophobic cavity can also selectively bind guests through various weak interactions. The archetypal non-functionalized resorcinarene has been exploited for many host-guest processes ranging from open inclusion, capsular assemblies, and nanotubes,[15–23] functionalization of this parent cavitand increases the scope of available constructs.

The 2-position of resorcinarenes is readily modified using electrophilic aromatic substitution.[24–28] Introducing suitable substituents at the 2-position can have a subtle yet significant effect on the macrocycles' guest binding properties. Indeed, in our previous reports, we have studied the binding properties of a series of resorcinarenes decorated at the 2-position with electron-donating ($CH_3$ or OH) and electron-withdrawing (Cl, Br, and I) groups with both tetramethyl ammonium and diquaternary ammonium [*N*,*N*-dialkyl-1,4-diazabicyclo[2.2.2]octane (alkyl2-DABCO)] halide salts.[29,30] Since cation-π interactions are believed to be the main host-guest interactions, enhanced binding was expected for resorcinarenes with electron-donating groups. Interestingly, enhanced

binding was instead observed for resorcinarenes with electron-withdrawing groups at the 2-position. We have demonstrated that this occurs because the electron-withdrawing groups render the phenolic hydrogens of the resorcinarenes more acidic, leading to stronger ion-pair binding. Evidently, phenol has pka of 10.0 whiles the 2-bromophenol derivative has a pka of 8.44.[31] In effect, the binding constant also increases as we increase the electron pull power of the substituent from I, to Br, to Cl.[29,30]

Phenoxide resorcinarenes are intermediates in the synthesis of alkylated derivatives. The tetra-deprotonated resorcinarene has been observed in solution, while mono- and di-deprotonated resorcinarenes have been isolated and characterized in the solid-state. However during our investigation of resorcinarene deprotonation with 1,4-diaminocyclohexane, we managed to produce a co-crystal consisiting of a mono- and tetra-deprotonated 2-methylresorcinarene and have characterized it crystallographically.[32] The 1,4-diaminocyclohexane, being a sufficiently strong base, abstracts protons from the resorcinarenes and subsequently acts as a cationic guest. The 1,4-diammoniumcyclohexane acting as a guest forms a dimeric charge-neutral capsule with the mono-deprotonated 2-methylresorcinarene and a tetra-deprotonated discrete assembly, with the 2-methylresorcinarene maintaining a $C_{4v}$ conformation.

Motivated by these reports, we hypothesized that having an electron-withdrawing group at the 2-position of the resorcinarene in the presence of a strong amine base will lead to multi-deprotonated resorcinarenes with enhanced binding of the subsequent cation. Additionally, the tetramethyl ammonium cation is well established to be structurally complementary with resorcinarenes' *endo*-cavity. In this contribution, we aim to investigate the following:

a) can a deprotonated resorcinarene with an electron-withdrawing bromine group on the 2-position be isolated in the solid state as a salt together with a corresponding protonated amine?

b) will the protonated amine form *endo*- or *exo*-cavity complexes with the deprotonated resorcinarenes?

c) will this charge-neutral salt still be capable of binding a tetramethyl ammonium cation?

To answer these questions, we attempted the solid state deprotonation and host-guest chemistry of 2-bromo-C-methyl-resorcinarene (**A2**) and amines (**B1**-**B7**) (Figure 1) in the presence and absence of tetramethylammonium chloride (**TMACl**), which resulted in two crystal structures. In the first example, we isolated the tri-deprotonated 2-bromo-C-methylresorcinarene ($\mathbf{A2}^{3-}$) and di-protonated dimethylpiperazine ($H_2\mathbf{B2}^{2+}$) as a dimeric capsule. In the second example, we isolated the bis-deprotonated 2-bromo-C-methylresorcinarene ($\mathbf{A2}^{2-}$) and $\mathbf{TMA}^{+}$ as a rigid nanotube with channels. X-ray crystallographic analyses was supplemented with $^{1}$H NMR and ITC experiments of one base (**B2**) to understand the thermodynamic differences between unfunctionalized, and 2-bromo-C-alkylresorcinarenes.

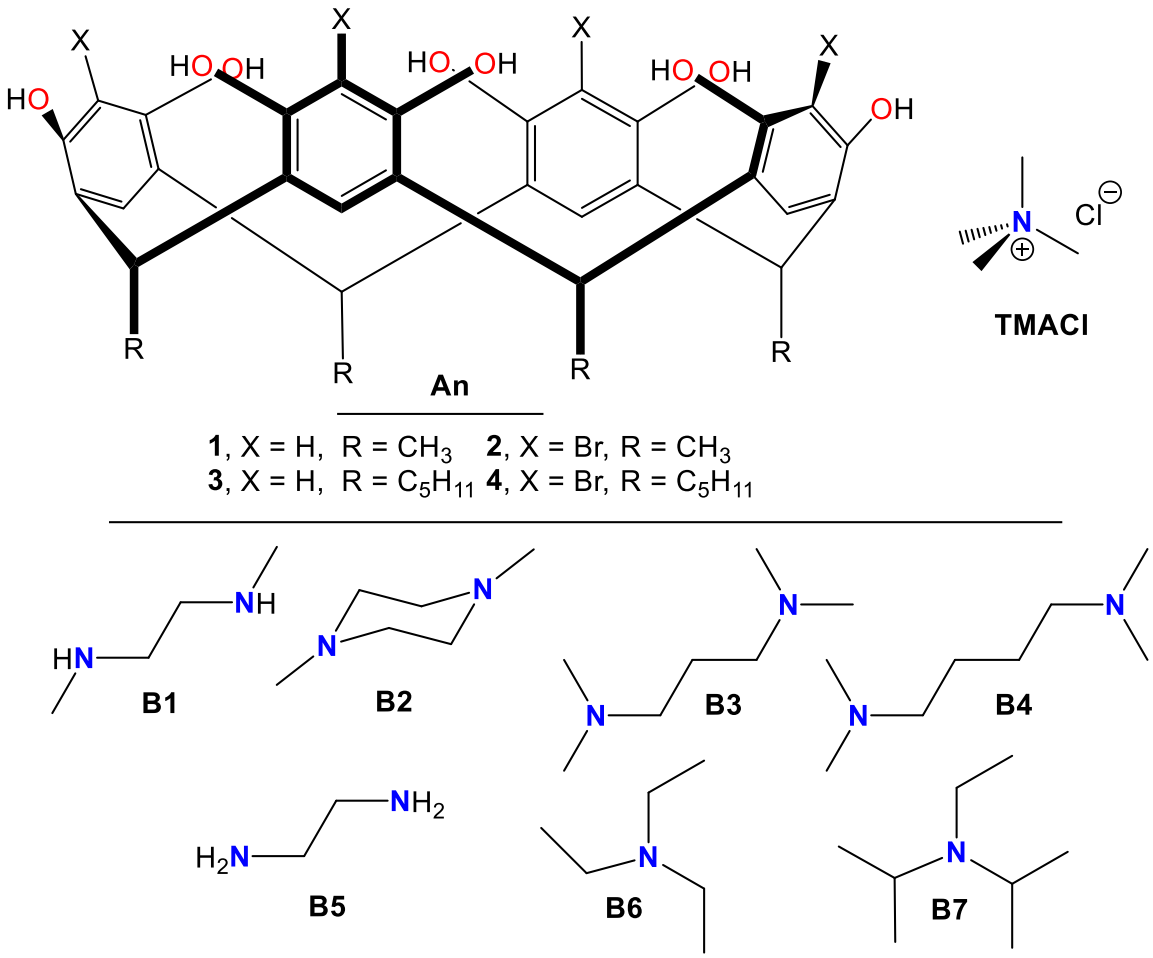


**Figure 1**. Chemical species used in the study: resorcinarene hosts **An** (**n** = **1-4**), amines **Bn** (*N,N'*-dimethylethylenediamine **B1**, *N,N'*-dimethylpiperazine **B2**, *N,N,N',N'*-tetramethylpropanediamine **B3**, *N,N,N',N'*-tetramethylbutanediamine **B4**, ethylenediamine **B5**, triethylamine **B6**, *N,N*-diisopropylethylamine **B7**), and tetramethylammonium chloride **TMACl**.

## RESULTS AND DISCUSSION

### X-Ray crystallography

Two host-guest crystal structures were obtained by using **A2**. Unfortunately, other attempts to crystallize host-guest complexes with **An** with the bases **Bn** and in the presence and absebnce of **TMACl** were unsuccessful. Complex **A2**+**B2** was obtained by mixing **A2**:**B2** in a 1:8 molar ratio in $CHCl_3$/MeOH. Slow evaporation of the reaction mixture afforded single crystals suitable for X-

ray diffraction. The complex **A2**+**B2** crystallizes in the triclinic space group *P*-1 and is a 2D coordination polymer, $[(\mathbf{A2})^{3-}\cdot(\mathrm{H}\mathbf{B2})^{+}\cdot(\mathrm{H_2}\mathbf{B2})^{2+}\cdot\mathrm{CH_3OH}\cdot\mathrm{CHCl_3}]_n$. The asymmetric unit consists of one triply deprotonated host ($\mathbf{A2}^{3-}$), one mono-protonated *exo*-dimethylpiperazine ($\mathrm{H}\mathbf{B2}^{+}$), half of a double protonated *exo*-dimethylpiperazine ($\mathrm{H_2}\mathbf{B2}^{2+}$), half of a double protonated *endo*-dimethylpiperazine ($\mathrm{H_2}\mathbf{B2}^{2+}$), one MeOH, and one disordered $\mathrm{CHCl_3}$ molecule (Figure S3, and see Supporting Information for additional detail). These are not perfectly symmetric molecular capsules, the two hosts are slightly offset (see Figure 2), but they still enclose their shared inner cavity. This cavity hosts one double protonated dimethylpiperazine ($\mathrm{H_2}\mathbf{B2}^{2+}$) and two methanol guest molecules. They are connected via N−H···O hydrogen bonds (d(O9···N1) = 2.608(5) Å) and the methanols are each bonded to a resorcinarene host (d(O6···O9) = 2.750(5) Å) effectively locking the dimeric capsule from the inside. Due to the size of the *endo*-$\mathrm{H_2}\mathbf{B2}^{2+}$ cation, the electron-rich interior of the capsule is almost fully occupied by the large $\mathrm{H_2}\mathbf{B2}^{2+}$ guest. The methanol molecules are only partly encapsulated leaving the methyl groups pointing towards the exterior of the capsule as well as the bromine groups of the hosts in an almost eclipsed position, leading to the Br···Br distance of 3.4191(7) Å (see CPK model in Figure 2). In addition to the N−H···O interactions of *endo*-$\mathrm{H_2}\mathbf{B2}^{2+}$, C−H···$\pi$ and C−H···Br contacts with the aromatic rings of the hosts were observed.

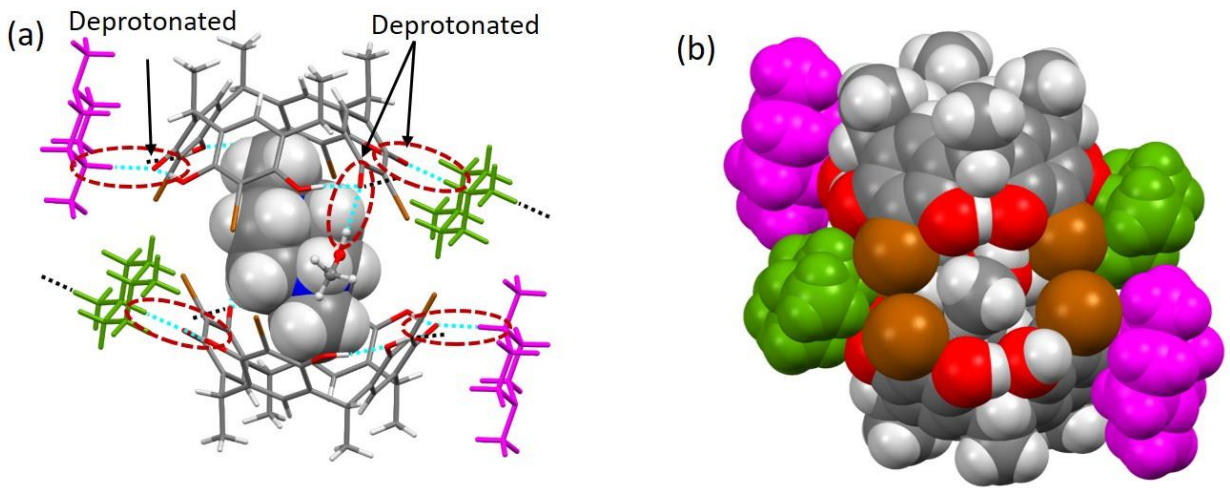


**Figure 2:** X-ray crystal structure of **A2**+**B2**. Left: Hosts (**A2**$^{3-}$) are represented in stick model, MeOH molecules in ball-and stick, *endo*-$H_2$**B2**$^{2+}$ in CPK model, bridging *exo*-$H_2$**B2**$^{2+}$ are in green color sticks, and terminal *exo*-H**B2**$^{+}$ in magenta color sticks; right: all in CPK model. Disordered, co-crystallized chloroform molecules have been omitted for clarity. Turquoise and black broken lines represent N−H···O and O−H···O hydrogen bonding, respectively.

Extension of the asymmetric unit reveals the formation of a hydrogen bonded 2D coordination polymer featuring dimeric capsules (see Figure 3). Two differentially protonated dimethylpiperazines are *exo*-cavity bound via N−H···O hydrogen bonds to the deprotonated oxygen atoms of the host. The first is a mono-protonated dimethylpiperazine (H**B2**$^{+}$, magenta), which acts as a terminal ligand; the second is a doubly protonated dimethylpiperazine ($H_2$**B2**$^{2+}$, green) whose cations act as linkers connect neighboring capsules into the higher-order linear structure. These two guests are bound on the opposite sides of the resorcinarene, and the resorcinarenes of the capsule adopt a head-to-tail arrangement relative to each other. This forms the 1D polymeric strand with bridging $H_2$**B2**$^{2+}$s along the *b*-axis (Figure 3a). The N···O distance between the host and bridging guest is slightly shorter (2.618(5) Å) than the one between host and

terminal guest (2.671(5) Å). The interaction between the resorcinarene hosts without the help of a linker is demonstrated in Figure 3(b). Here, the capsules are connected directly via O−H···O hydrogen bonds (2.547(4) Å) forming an extended 2D polymeric assembly. The polar and apolar layers alternate along the *c*-axis.

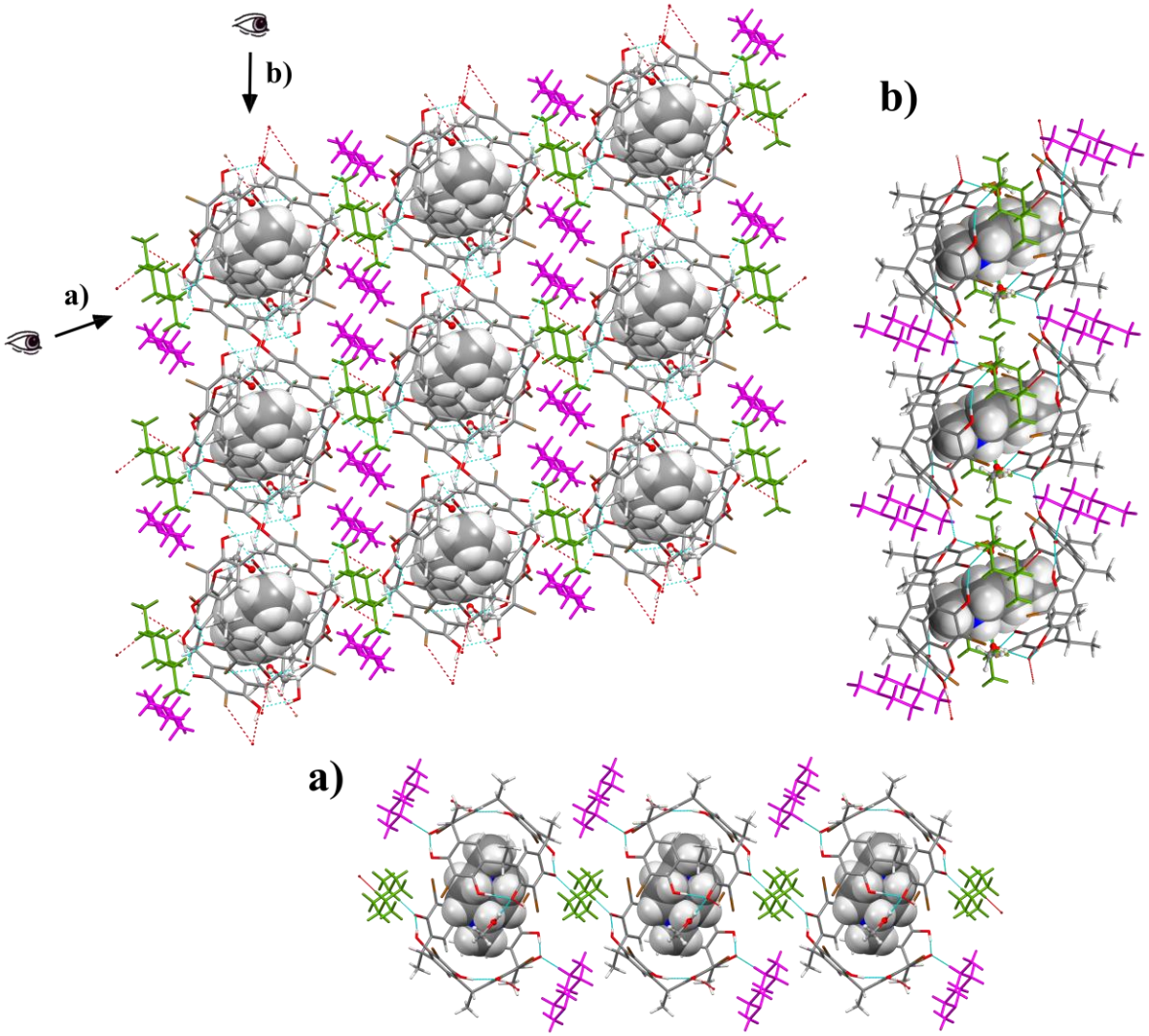


**Figure 3:** 2D hydrogen-bonded polymer viewed along the *ab* plane (top left): (a) capsules are linked together via bridging $H_2$**B2**$^{2+}$ molecules along the *b*-axis, (b) hydrogen bonds connect the capsules directly along the *a*-axis. Disordered, co-crystallized chloroform molecules have been

omitted for clarity. Turquoise and red broken lines represent N−H···O and O−H···O hydrogen bonding, respectively.

The initial host-guest complexation of **A2**+**B1** did not afford single crystals suitable for X-ray diffraction. The addition of excess tetramethylammonium chloride to the reaction mixture resulted in the new host-guest complex of the type $[(\mathbf{A2})^{2-}\cdot 2(\mathbf{TMA})^{+}\cdot x CH_3OH\cdot y H_2O]_n$. Similar to the previous structure, this complex was obtained from $CHCl_3$/MeOH via slow evaporation at ambient temperature. It crystallizes in the trigonal space group $R\bar{3}$ with Z = 18. The asymmetric unit consists of one doubly deprotonated host molecule ($\mathbf{A2}^{2-}$), one disordered *endo*-$\mathbf{TMA}^{+}$ cation, one disordered *exo*-$\mathbf{TMA}^{+}$ cation, and highly disordered co-crystallized solvent molecules (see Figure 4). The latter have been squeezed out from the final structure model with the SQUEEZE[33] procedure in PLATON.[34,35] No chlorides or protonated *N,N'*-dimethylethylenediamines (**B1**) could be observed in this solid-state structure. The formation of this product can be explained as follows: the base **B1** initially deprotonates the 2-bromo-C-methylresorcinarene; after addition of excess **TMACl**, the protonated **B1** is replaced by the smaller and more suitable guest, the $\mathbf{TMA}^{+}$ cation. Unlike the capsule discussed above, these molecules self-assemble into a nanotube, stabilized via several O−H···O hydrogen bonds between the resorcinarenes (see Figure 5). The nanotube has a diameter of ca. 6 Å. Additional stabilizing intermolecular C−H···$\pi$ interactions between the *endo*-$\mathbf{TMA}^{+}$ cations with the aromatic rings of the hosts were observed.

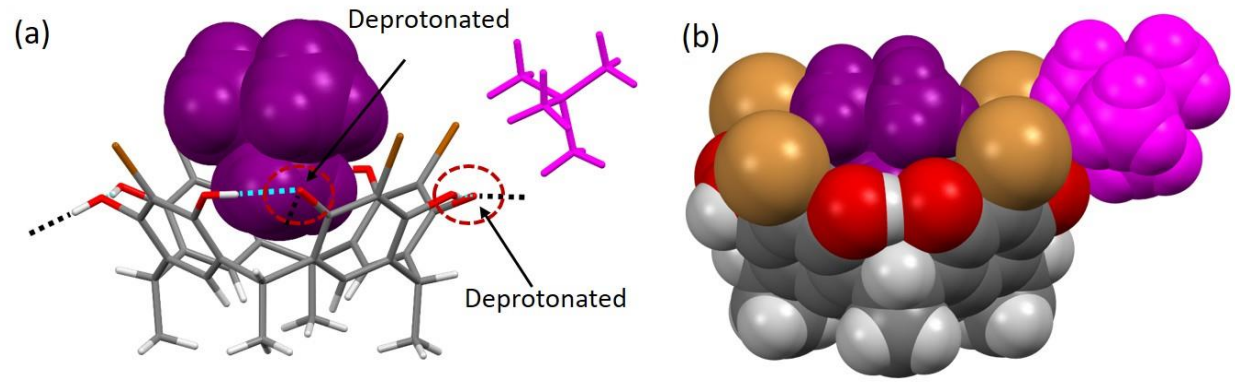


**Figure 4:** X-ray crystal structure of **A2•TMA** obtained from a mixture of **A2**+**B1**+**TMACl**. (a) Host (**A2**$^{2-}$) is represented in a stick model, *endo*-**TMA**$^{+}$ in the purple CPK model, and *exo*-**TMA**$^{+}$ in as the magenta stick. Atom sites of tetramethylammonium cations with minor occupancies have been omitted for clarity. Turquoise and black broken lines represent O−H···O hydrogen bonding. The deprotonated phenolic groups are indicated. (b) All in CPK model.

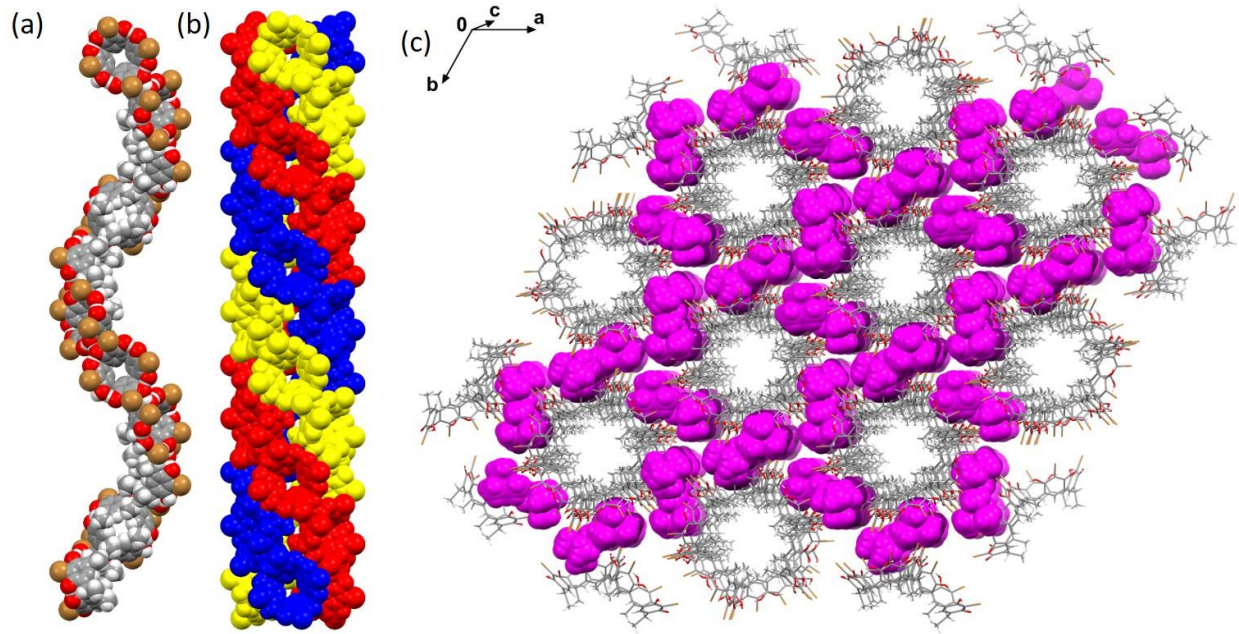

**Figure 5:** Di-deprotonated 2-bromo-C-methylresorcinarenes form nanotubes along the *c*-axis through hydrogen bonds: (a) adjacent resorcinarenes are connected to each other forming a single helix, (b) the resorcinarene triple helix tube, and (c) crystal packing of **A2•TMA**.

**Solution studies**

To probe the solution dynamics of these processes, we conducted NMR and isothermal titration calorimetry (ITC) experiments with *N,N'*-dimethylpiperazine **B2** since this was the only base that crystallized as discussed above. The crystal structures were obtained with simple methyl-functionalized lower rin resorcinarenes (**A1** and **A2**), but these species are challenging to study in solution due to the significant 'breathing' flexibility of the hydrophobic cavity and their limited solubility in chloroform.[36] Consequently to examine the robustness of this salt formation, we switched to employing the more configurationally stable pentyl derivatives **A3** (unfunctionalized at C-2) and **A4** (brominated at C-2, Figure 1). The host-guest chemistry between each of these receptors, **B2** (the dimethyl piperazine base), and **TMACl** (a salt) were probed in solution through $^1$H NMR and ITC measurements. Halogenation, by decreasing electron density in the ring, increases the acidity of the phenolic hydroxyl groups which has a significant influence on the ion-pair binding of ammonium salts in solution.[29] We explored the deprotonation and host-guest complexation of these receptors by monitoring the shielding and deshielding effects on **TMA**$^+$, **B2**, **A3**, and **A4**'s proton signals. The complexes in solution are in rapid equilibrium with the free components, hence only one set of signals representing an average of the overall host-guest system is observed. In $CDCl_3/CD_3OD$ (90/10 v/v), with the methanol needed to fully dissolve the species at a concentration suitable for NMR, the chemical shift changes of the receptors' aryl hydrogens were minimal due to the limited flexibility of the long chain macrocycles[36] and the perfect size-

match of the **TMA**$^+$ which prevents the need for the distortion of the cavity to accommodate the guest.

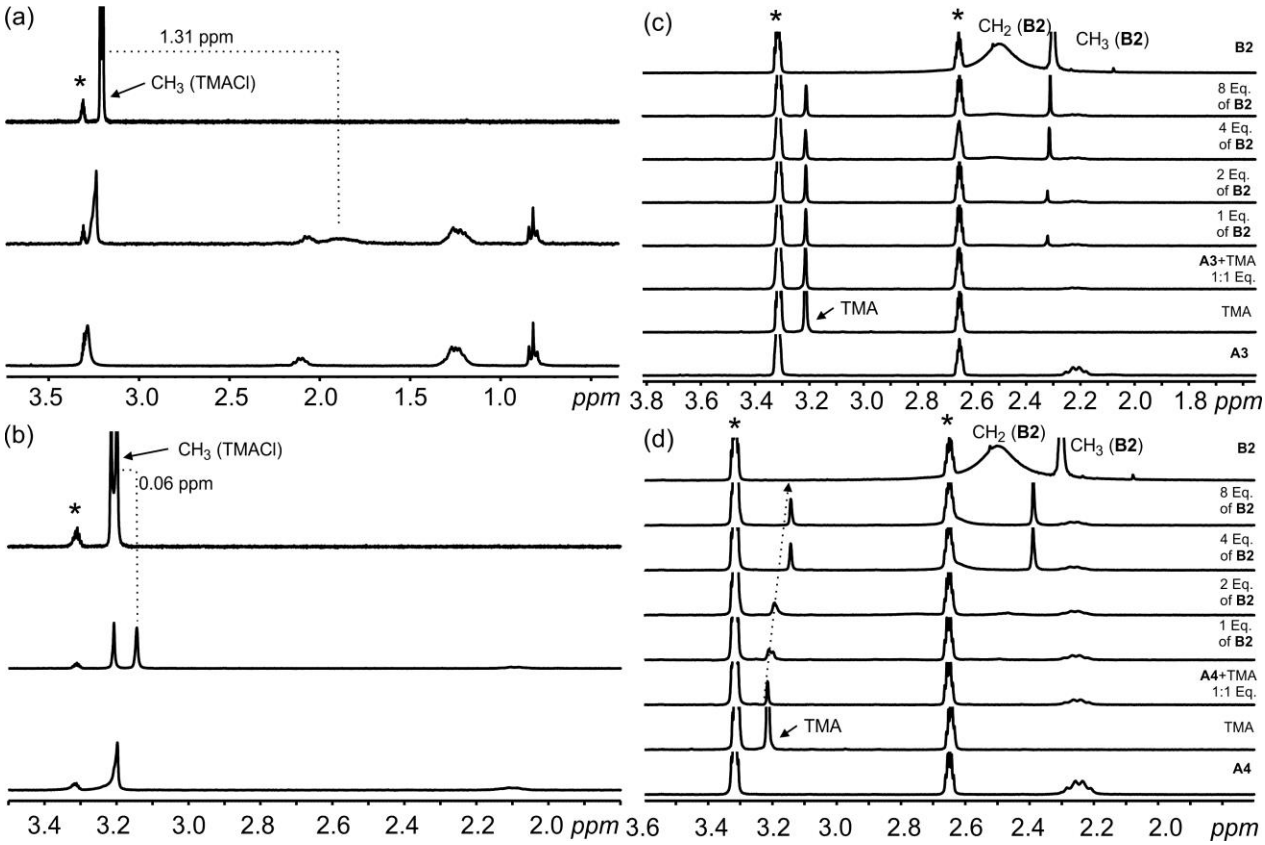


**Figure 6**: $^1$H NMR stack spectra (90% $CDCl_3$, 10% $CD_3OD$, 298 K) showing: (a) pure TMACl (top), equimolar **TMACl@A3** (middle), pure **A3** (bottom); (b) pure **TMACl** (top), equimolar **TMACl@A4** (middle), pure **A4** (bottom). $^1$H NMR stack spectra (70% $CD_3OD$, 30% DMSO-$d_6$, 298 K) showing the addition of up to 8 quivalents of **B2** to an equimolar mixture of (c) **A3**+**TMA**, and (d) **A4**+**TMA**. Star represents the residual solvent. The dash lines give an indication of the signal changes in ppm.

By following the extent of shielding, we qualitatively determine how deep the **TMA**$^+$ sits in the cavity of the receptor, but not the binding affinity (see the section on ITC below).[37] In this solvent mixture, **TMA**$^+$ is highly shielded in the parent resorcinarene (**A3**) compared to halogenated

resorcinarene (**A4**) (Figure 6a and 6b). As an average of an overall system, the decreased electron density of the **A4** cavity compared to **A3** also reduces the degree of shielding observed. Introduction of the base, **B2** in $CDCl_3$ deprotonates the resorcinarene and is accompanied by the disappearance of the Aryl-OH groups (Figure S5); however, the loss of the Ar-OH signals could also be a result of a fast exchange of another form. To further probe the effect of deprotonation, **B2** was titrated into an equimolar mixture of the host and $\mathbf{TMA}^+$ in $CD_3OD$/DMSO-$d_6$ (70/30 v/v at 298 K). This highly polar solvent mixture would better separate the ion-pairing of the deprotonated host. Considering the extreme competition of this solvent mixture, only minor shielding of the $\mathbf{TMA}^+$ proton signals is observed which is expected. In the case of **A3**+$\mathbf{TMA}^+$, the addition of **B2** to this equimolar mixture did not indicate any changes to either the host's or the $\mathbf{TMA}^+$'s signals. (Figure 6c, Figure S6), and only very minimal changes to the **B2** signals were observed. This suggests limited proton transfer. In the case of **A4**+$\mathbf{TMA}^+$, the addition of **B2** resulted in a significant shielding of $\mathbf{TMA}^+$'s signal. The host aryl signal also changes significantly supporting deprotonation and host-guest complexation (Figure 6c, Figure S6). Additionally, clear deshielding of the **B2** signals points to the protonation of this species under this condition. This result also supports the phenomenon seen with the crystal nanotube structure obtained from **A2**+**B1**+**TMACl**, where the base deprotonates the host and makes it a better receptor for the **TMA** cation.

Next, we used Isothermal calorimetric titrations between receptors **A3**, **A4**, dimethyl piperazine (**B2**), and tetramethylammonium chloride (**TMACl**) to quantify the thermodynamic parameters of binding including the affinity constants (Ka), and the enthalpic and entropic contributions to the self-assembly processes in solution. These titrations were carried out in chloroform to ensure optimum deprotonation of the acidic hydroxyl groups of the resorcinarene by the base and

enhanced host-guest binding. In solution and solid-state, prior research has shown that up to four hydroxyl groups can be deprotonated by a suitable base.[38–41] Deprotonation by dimethyl piperazine (**B2**) creates a cationic guest ($H_2$**B2**$^{2+}$) in solution that can occupy the cavity of the resorcinarene, stabilized through cation-π interactions. The electron withdrawing bromo-substituent at position 2 of the resorcinarene **A4** decreases electron density in the ring and as a result, we observed a weaker binding affinity of the $H_2$**B2**$^{2+}$ in the cavity of the resorcinarene **A4** compared to **A3** (Table 1, Figure S7, S8). However, the thermodynamics of $H_2$**B2**$^{2+}$ *endo*-complexation in **A3** is mostly driven by entropy, while the *endo*-complexation in **A4** is driven by enthalpy to create a more spontaneous system. We also observed a second binding event in **B2@A3** that possibly involves a second resorcinarene.

In calorimetric titrations with **TMACl**, a salt, the deprotonation event does not occur, but what happens is a host-guest ion-pair binding also observed with unfunctionalized resorcinarenes.[30,32] It is noteworthy that the reduced binding affinity of **A4** towards the **TMA**$^+$ cation due to the decreased cavity electron density is compensated by the increased binding affinity of the chloride anion to the more acidic phenolic hydrogens. This was reflected by the higher order of magnitude binding of $K_1$ and $K_2$ in **TMACl@A4** compared to **TMACl@A3**. This is the synergistic effect created by the interaction of the **A4** with the chloride counterion of **TMACl** through enhanced hydrogen bonding. The resultant **TMA**$^+$ is much more readily available to undergo cation-π interactions with the resorcinarene cavity. Both molecular recognition processes ($K_1$ and $K_2$) are enthalpically and entropically favourable but complexation is slightly stronger in **A4** compared to **A3**.

**Table 1:** Thermodynamic binding parameters of formed complexes between the receptors **A3** and **A4** and the guests (**B2** and **TMACl**) by ITC[a]

| **Complex** | $K_1$ | $\Delta H_1$ | $T\Delta S_1$ | $\Delta G_1$ |
|---|---|---|---|---|
| | **(× $10^5$) $M^{-1}$** | **kcal/mol** | **kcal/mol** | **kcal/mol** |
| **A3@B2** | 0.87±0.07 | -10.8±2.13 | -4.08 | -6.72 |
| **A4@B2** | 0.11±0.002 | -12.1±2.16 | -6.53 | -5.57 |
| **A3@TMACl** | 0.51±0.15 | 0.25±0.06 | 6.68 | -6.43 |
| **A4@TMACl** | 3.63±1.15 | -0.32±0.11 | 7.54 | -7.86 |
| **Complex** | $K_2$ | $\Delta H_2$ | $T\Delta S_2$ | $\Delta G_2$ |
| | **(× $10^4$) $M^{-1}$** | **kcal/mol** | **kcal/mol** | **kcal/mol** |
| **A3@B2** | 0.30±0.05 | -125.4±6.33 | -120.7 | -4.70 |
| **A4@B2** | * | * | * | * |
| **A3@TMACl** | 0.13±0.006 | -8.51±2.48 | -4.23 | -4.28 |
| **A4@TMACl** | 2.32±0.54 | -6.81±0.62 | -0.86 | -5.95 |

[a] ITC was done in chloroform at 298K. * fit to only one site binding model

## CONCLUSIONS

In conclusion, in the presence of amine bases, the 2-bromo-C-methylresorcinarene host can be doubly and triply deprotonated resulting in host-guest complexes in the solid phase. In the triply deprotonated host, the doubly protonated amine acts as a guest in a dimeric capsular assembly with another protonated amine connecting the complexes into a 2D network of dimeric capsules. In the doubly deprotonated host, and in the presence of **TMACl**, a host-guest assembly of only the deprotonated host and the $\mathbf{TMA}^+$ cation was isolated resulting in a tightly packed nanotube. $^1$H NMR solution studies with one base, support the deprotonation and host-guest complexation of the brominated resorcinarenes with more acidic protons that are easily deprotonated by the base. ITC studies provide an overview of the thermodynamics of the binding process with the system

being either enthalpy or entropy driven depending on the substituent on the resorcinarene ring. Quantification reveals a very high binding constant for **TMACl** by the 2-bromo-C-pentylresorcinarene ($K_1$=3.63×10$^5$ M$^{-1}$, $K_2$=2.32×10$^4$ M$^{-1}$), much higher than with unfunctionalized C-pentylresorcinarene ($K_1$=5.10×10$^4$ M$^{-1}$, $K_2$=1.30×10$^3$ M$^{-1}$) which we attribute to stronger ion-pair binding involving the more acidic phenolic hydroxyl groups. This work provides additional fundamental insights into how subtle changes on the resorcinarenes can have a fundamental effect on their capability as synthons in the construction of very exotic supramolecular architectures.

## EXPERIMENTAL SECTION

The solvents used for synthesis, $^1$H NMR and ITC experiments, and crystallization experiments were reagent grade and were used as received without further purification. Receptors **A1 – A4** were synthesized by following literature methods.[42,43] The amines **B1-B7** and **TMACl** were purchased from Sigma Aldrich. $^1$H NMR spectra were recorded on a Bruker Avance DRX 300 spectrometer. ITC measurements were performed using VP-ITC instrument made by MicroCal.

Single-crystal X-ray data for **A2**+**B2** (CCDC-2156196) and **A2**+**B1**+**TMACl** (CCDC-2156197) were collected using Bruker-Nonius KappaCCD diffractometer with an APEX-II detector with graphite-monochromatized Mo-$K_\alpha$ ($\lambda$ = 0.71073 Å) radiation. Data collection and reduction were performed using the program *COLLECT*[44] and *HKL DENZO AND SCALEPACK*,[45] respectively, and the intensities were corrected for absorption using *SADABS*.[46] The structures were solved with Direct Methods (*SHELXS*)[47–49] and refined by full-matrix least-squares based on $F^2$ using *SHELXL*-2015. Single-crystal X-ray data and experimental details are given in the Supporting Information.

## ASSOCIATED CONTENT

**Supporting Information**. The Supporting Information is available free of charge on the ACS Publication website. X-Ray experimental details, 1H NMR, and ITC details are included in the Supporting Information.


## ACKNOWLEDGMENT

The authors gratefully acknowledge financial support from the American Chemical Society (NKB: ACS-PRF grant no. 39427), Oakland University, MI, USA, the Academy of Finland (KR: grant no. 298817), and the University of Jyväskylä. We also acknowledge the financial support from the Natural Sciences and Engineering Research Council of Canada (JFT: grant no. 2018-06338), and the Ontario Early Researcher Award (JFT: grant no. ER18-14-114).


## REFERENCES


(1) Puttreddy, R.; Beyeh, N. K.; Rissanen, K. Conformational Changes in C Methyl - Resorcinarene Pyridine N -Oxide Inclusion Complexes in the Solid State. *CrystEngComm* **2016**, *18* (26), 4971–4976. https://doi.org/10.1039/C6CE00240D.

(2) Twum, K.; Schileru, N.; Elias, B.; Feder, J.; Yaqoo, L.; Puttreddy, R.; Szczesniak, M. M.; Beyeh, N. K. Water Soluble Host–Guest Chemistry Involving Aromatic N-Oxides and Sulfonateresorcinarene. *Symmetry 2020, Vol. 12, Page 1751* **2020**, *12* (11), 1751. https://doi.org/10.3390/SYM12111751.

(3) Kodiah Beyeh, N.; Aumanen, J.; Åhman, A.; Luostarinen, M.; Mansikkamäki, H.; Nissinen, M.; Korppi-Tommola, J.; Rissanen, K. Dansylated Resorcinarenes. *New Journal of Chemistry* **2007**, *31* (3), 370–376. https://doi.org/10.1039/B615772F.

(4) Borowiak, T.; Aczy´nski, M. ,; Aczy´nski, A.; Pietraszkiewicz, M.; Pietraszkiewicz, O. Structural Study of C-Undecylcalix[4]Resorcinarene Solvate with Dioxane. *Journal of inclusion phenomena and macrocyclic chemistry 1999 35:1* **1999**, *35* (1), 131–138. https://doi.org/10.1023/A:1008115002434.

(5) Twum, K.; Rissanen, K.; Beyeh, N. K. Recent Advances in Halogen Bonded Assemblies with Resorcin[4]Arenes. *The Chemical Record* **2021**, *21* (2), 386–395. https://doi.org/10.1002/TCR.202000140.

(6) Gunter, M.; Society, M. J.-J. of the C.; Perkin, undefined; 1994, undefined. Porphyrin–Crown Ether Macrotricyclic Co-Receptors for Bipyridinium Cations. *pubs.rsc.org*.

(7) Kang, J.; Rebek, J. Acceleration of a Diels–Alder Reaction by a Self-Assembled Molecular Capsule. *Nature 1997 385:6611* **1997**, *385* (6611), 50–52. https://doi.org/10.1038/385050a0.

(8) Conn, M. M.; Rebek, J. Self-Assembling Capsules. *Chemical Reviews* **1997**, *97* (5), 1647–1668. https://doi.org/10.1021/CR9603800.

(9) Boerrigter, H.; Verboom, W.; van Hummel, G. J.; Harkema, S.; Reinhoudt, D. N. Selective Functionalization of Resorcinarene Cavitands; Single Crystal X-Ray Structure of a Distally Functionalized Cavitand. *Tetrahedron Letters* **1996**, *37* (29), 5167–5170. https://doi.org/10.1016/0040-4039(96)01027-1.

(10) Behboodi-Sadabad, F.; Trouillet, V.; Welle, A.; Messersmith, P. B.; Levkin, P. A. Surface Functionalization and Patterning by Multifunctional Resorcinarenes. *ACS Applied Materials and Interfaces* **2018**, *10* (45), 39268–39278. https://doi.org/10.1021/ACSAMI.8B14771/SUPPL_FILE/AM8B14771_SI_002.AVI.

(11) Balasubramanian, R.; Kwon, Y. G.; Wei, A. Encapsulation and Functionalization of Nanoparticles in Crosslinked Resorcinarene Shells. *Journal of Materials Chemistry* **2006**, *17* (1), 105–112. https://doi.org/10.1039/B614295H.

(12) Yao, Y.; Sun, Y.; Han, Y.; Yan, C. Preparation of Resorcinarene-Functionalized Gold Nanoparticles and Their Catalytic Activities for Reduction of Aromatic Nitro Compounds. *Chinese Journal of Chemistry* **2010**, *28* (5), 705–712. https://doi.org/10.1002/CJOC.201090135.

(13) Chen, J.; Körner, S.; Craig, S. L.; Rudkevich, D. M.; Rebek, J. Amplification by Compartmentalization. *Nature 2002 415:6870* **2002**, *415* (6870), 385–386. https://doi.org/10.1038/415385b.

(14) Ito, H.; Kusukawa, T.; Fujita, M. Wacker Oxidation in an Aqueous Phase through the Reverse Phase-Transfer Catalysis of a Self-Assembled Nanocage. *http://dx.doi.org/10.1246/cl.2000.598* **2004**, No. 6, 598–599. https://doi.org/10.1246/CL.2000.598.

(15) Hayashida, O.; Uchiyama, M. Cyclophane-Based Tetra(Resorcinarene) as a Host for Both Histone and Hydrophobic Molecular Guests. *Tetrahedron Letters* **2006**, *47* (24), 4091–4094. https://doi.org/10.1016/J.TETLET.2006.03.170.

(16) Kodiah Beyeh, N.; Ala-Korpi, A.; Cetina, M.; Valkonen, A.; Rissanen, K. Recognition of N-Alkyl and N-Aryl Acetamides by N-Alkyl Ammonium Resorcinarene Chlorides. *Chemistry – A European Journal* **2014**, *20* (46), 15144–15150. https://doi.org/10.1002/CHEM.201402533.

(17) Beyeh, N. K.; Ala-Korpi, A.; Pan, F.; Jo, H. H.; Anslyn, E. v.; Rissanen, K. Cooperative Binding of Divalent Diamides by N-Alkyl Ammonium Resorcinarene Chlorides. *Chemistry – A European Journal* **2015**, *21* (26), 9556–9562. https://doi.org/10.1002/CHEM.201406504.

(18) research, J. R. J.-A. of chemical; 2009, undefined. Molecular Behavior in Small Spaces. *ACS Publications* **1660**, *42* (10), 48. https://doi.org/10.1021/ar9001203.

(19) Avram, L.; Cohen, Y. Hexameric Capsules of Lipophilic Pyrogallolarene and Resorcinarene in Solutions as Probed by Diffusion NMR: One Hydroxyl Makes the Difference. *Organic Letters* **2003**, *5* (18), 3329–3332. https://doi.org/10.1021/OL035211Y/SUPPL_FILE/OL035211YSI20030730_095740.PDF.

(20) Shivanyuk, A.; Rebek, J. Assembly of Resorcinarene Capsules in Wet Solvents. *J Am Chem Soc* **2003**, *125* (12), 3432–3433. https://doi.org/10.1021/JA027982N/ASSET/IMAGES/JA027982N.SOCIAL.JPEG_V03.

(21) Avram, L.; Cohen, Y. Spontaneous Formation of Hexameric Resorcinarene Capsule in Chloroform Solution as Detected by Diffusion NMR. *J Am Chem Soc* **2002**, *124* (51), 15148–15149. https://doi.org/10.1021/JA0272686/ASSET/IMAGES/JA0272686.SOCIAL.JPEG_V03.

(22) Evan-Salem, T.; Cohen, Y. Octahydroxypyridine[4]Arene Self-Assembles Spontaneously to Form Hexameric Capsules and Dimeric Aggregates. *Chemistry - A European Journal* **2007**, *13* (27), 7659–7663. https://doi.org/10.1002/CHEM.200700461.

(23) Avram, L.; Cohen, Y. Discrimination of Guests Encapsulation in Large Hexameric Molecular Capsules in Solution: Pyrogallol[4]Arene versus Resorcin[4]Arene Capsules. *J Am Chem Soc* **2003**, *125* (52), 16180–16181. https://doi.org/10.1021/JA0377394/SUPPL_FILE/JA0377394SI20031104_113713.PDF.

(24) Beyeh, N. K.; Rissanen, K. N-Alkyl Ammonium Resorcinarene Salts: A Versatile Family of Calixarene-Related Host Molecules. In *Calixarenes and Beyond*; Springer, 2016; pp 255–284. https://doi.org/10.1007/978-3-319-31867-7_11.

(25) Beyeh, N. K.; Valkonen, A.; Bhowmik, S.; Pan, F.; Rissanen, K. N-Alkyl Ammonium Resorcinarene Salts: Multivalent Halogen-Bonded Deep-Cavity Cavitands. *Organic Chemistry Frontiers* **2015**, *2* (4), 340–345. https://doi.org/10.1039/c4qo00326h.

(26) Pan, F.; Beyeh, N. K.; Rissanen, K. Concerted Halogen-Bonded Networks with N-Alkyl Ammonium Resorcinarene Bromides: From Dimeric Dumbbell to Capsular Architectures. *J Am Chem Soc* **2015**, *137* (32), 10406–10413. https://doi.org/10.1021/jacs.5b06590.

(27) Ueda, M.; Takahashi, D.; Nakayama, T.; Haba, O. Three-Component Negative-Type Photoresist Based on Calix[4]Resorcinarene, a Cross-Linker, and a Photoacid Generator. *Chemistry of Materials* **1998**, *10* (8), 2230–2234. https://doi.org/10.1021/CM980166N.

(28) Nakayama, T. A New Three-Component Photoresist Based on Calix[4]Resorcinarene Derivative, a Cross-Linker, and a Photo-Acid Generator. *Bull Chem Soc Jpn* **1998**, *71* (12), 2979–2984. https://doi.org/10.1246/BCSJ.71.2979.

(29) Beyeh, N. K.; Weimann, D. P.; Kaufmann, L.; Schalley, C. A.; Rissanen, K. Ion-Pair Recognition of Tetramethylammonium Salts by Halogenated Resorcinarenes. *Chemistry – A European Journal* **2012**, *18* (18), 5552–5557. https://doi.org/10.1002/CHEM.201103991.

(30) Kodiah Beyeh, N.; Göth, M.; Kaufmann, L.; Schalley, C. A.; Rissanen, K. The Synergetic Interplay of Weak Interactions in the Ion-Pair Recognition of Quaternary and Diquaternary Ammonium Salts by Halogenated Resorcinarenes. *European Journal of Organic Chemistry* **2014**, *2014* (1), 80–85. https://doi.org/10.1002/EJOC.201300886.

(31) Tee, O. S.; Paventi, M.; Bennett, J. M. Kinetics and Mechanism of the Bromination of Phenols and Phenoxide Ions in Aqueous Solution. Diffusion-Controlled Rates. *J Am Chem Soc* **1989**, *111* (6), 2233–2240. https://doi.org/10.1021/JA00188A044/SUPPL_FILE/JA00188A044_SI_001.PDF.

(32) Puttreddy, R.; Beyeh, N. K.; Kalenius, E.; Ras, R. H. A.; Rissanen, K. 2-Methylresorcinarene: A Very High Packing Coefficient in a Mono-Anion Based Dimeric Capsule and the X-Ray Crystal Structure of the Tetra-Anion. *Chemical Communications* **2016**, *52* (52), 8115–8118. https://doi.org/10.1039/C6CC03289C.

(33) van der Sluis, P.; Spek, A. L. BYPASS: An Effective Method for the Refinement of Crystal Structures Containing Disordered Solvent Regions. *Acta Cryst,* **1990**, *46* (3), 194–201. https://doi.org/10.1107/S0108767389011189.

(34) Spek, A. L.; IUCr. Single-Crystal Structure Validation with the Program PLATON. *urn:issn:0021-8898* **2003**, *36* (1), 7–13. https://doi.org/10.1107/S0021889802022112.

(35) Spek, A. L. Structure Validation in Chemical Crystallography. *Acta Crystallogr. D. Biol Crystallogr.* **2009**, *65* (2), 148–155. https://doi.org/10.1107/S090744490804362X.

(36) Twum, K.; Rautiainen, J. M.; Yu, S.; Truong, K. N.; Feder, J.; Rissanen, K.; Puttreddy, R.; Beyeh, N. K. Host-Guest Interactions of Sodiumsulfonatomethyleneresorcinarene and Quaternary Ammonium Halides: An Experimental-Computational Analysis of the Guest Inclusion Properties. *Crystal Growth and Design* **2020**, *20* (4), 2367–2376. https://doi.org/10.1021/acs.cgd.9b01540.

(37) Kwaku Twum; Sadraei, S. I.; Jordan Feder; Maryamdokht Taimoory, S.; Kari Rissanen; F. Trant, J.; Kodiah Beyeh, N. Sharing the Salt Bowl: Counterion Identity Drives N -Alkyl Resorcinarene Affinity for Pyrophosphate in Water. *Organic Chemistry Frontiers* **2022**, *9* (5), 1267–1275. https://doi.org/10.1039/D1QO01877A.

(38) Farina, F.; Talotta, C.; Gaeta, C.; Neri, P. Regioselective O-Substitution of C-Undecylresorcin[4]Arene. *Organic Letters* **2011**, *13* (18), 4842–4845. https://doi.org/10.1021/OL201919P/SUPPL_FILE/OL201919P_SI_001.PDF.

(39) Jasat, A.; Sherman, J. C. Carceplexes and Hemicarceplexes. *Chem Rev* **1999**, *99* (4). https://doi.org/10.1021/CR960048O.

(40) Schneider, H. -J; Güttes, D.; Schneider, U. A Macrobicyclic Polyphenoxide as Receptor Analogue for Choline and Related Ammonium Compounds. *Angewandte Chemie*

*International Edition in English* **1986**, *25* (7), 647–649. https://doi.org/10.1002/ANIE.198606471.

(41) Puttreddy, R.; Beyeh, N. K.; Kalenius, E.; Ras, R. H. A.; Rissanen, K. 2-Methylresorcinarene: A Very High Packing Coefficient in a Mono-Anion Based Dimeric Capsule and the X-Ray Crystal Structure of the Tetra-Anion. *Chemical Communications* **2016**, *52* (52), 8115–8118. https://doi.org/10.1039/C6CC03289C.

(42) Jasat, A.; Sherman, J. C. Carceplexes and Hemicarceplexes. *Chem Rev* **1999**, *99* (4). https://doi.org/10.1021/CR960048O.

(43) Timmerman, P.; Verboom, W.; Reinhoudt, D. N. Resorcinarenes. *Tetrahedron* **1996**, *52* (8), 2663–2704. https://doi.org/10.1016/0040-4020(95)00984-1.

(44) Hooft R.W.W. COLLECT Nonius BV Delft The Netherlands. Acta Crystallographica Section E Structure Reports 1998.

(45) Otwinowski, Z.; Minor, W. [20] Processing of X-Ray Diffraction Data Collected in Oscillation Mode. *Methods in Enzymology* **1997**, *276*, 307–326. https://doi.org/10.1016/S0076-6879(97)76066-X.

(46) Sheldrick G.M. SADABS. University of Göttingen, Germany 1996.

(47) Sheldrick, G. M. Crystal Structure Refinement with SHELXL. *Acta Cryst.* **2015**, *71* (1), 3–8. https://doi.org/10.1107/S2053229614024218.

(48) Sheldrick G.M. SHELXL13. University of Gottingen, Germany 2013.

(49) Sheldrick, G. M. A Short History of ShelXL. *Acta Cryst.* **2008**, *A64*, 112–122.

**FOR TABLE OF CONTENTS ONLY**

Multi-deprotonated 2-bromo-C-alkylresorcinarene forms host-guest complexes with both protonated dimethylpiperazine and tetramethylammonium cations resulting in capsular and nanotube assemblies. Increased ion-pair binding is attributed to the electron-withdrawing abilities of the bromine rendering the hydroxyl groups acidic for anion binding.